ISSN NO. 2320-5407

Journal Homepage: -www.journalijar.com

INTERNATIONAL JOURNAL OF ADVANCED RESEARCH (IJAR)

Article DOI:10.21474/IJAR01/1184
DOI URL: http://dx.doi.org/10.21474/IJAR01/1184

RESEARCH ARTICLE

STRUCTURAL CHARACTERIZATION AND ELECTRICAL PROPERTIES OF a- S/Sb RATIO THIN FILMS.

N.M. Abdel-Moniem.
Faculty of Science, Tanta University, Egypt.

Manuscript Info

Manuscript History

Received: 15 June 2016
Final Accepted: 18 July 2016
Published: August 2016

Key words:
amorphous,Sb, S, films, crystal, conductivity, structure.

Abstract

Thin films of amorphous Sb_xS_{100-x} (x=10, 20, 30 and 40 at %) were prepared by thermal evaporation technique. The films were annealed at 510K for 2h, and investigated by X-ray diffraction patterns. The results showed a crystallization of the annealed films with different degrees depending on the access of the coordination number due to Sb substitution in S atoms. Electrical conductivity measurements were carried out on as-deposited and annealed films in the temperature range 300-600K. The results indicated that the conductivity of the annealed films is higher than as-deposited films, which confirms the transformation of the amorphous films to a crystalline state as derived from X-ray diffraction analysis. The obtained results were explained according to the presence of nucleation centers for crystallization due to Sb substitution in S atoms which grows by annealing.

Introduction:

The studies of chalcogenide had interested because of their applications in the electronic devices such as photoconductivity targets of television cameras [1]. Chalcogenide glasses had received much attention due to their potential use in varies solid state devices. The nature of the localized states and gap states in their semiconductors is fundamental for a better understanding of the electrical properties [2]. The use of thin films polycrystalline semiconductor has attracted much interest in an expanding variety of applications in various electronic and optoelectronic devices. The technological interest in polycrystalline based devices is mainly caused by their very low production costs. Thin films occupy a prominent place in basic research and solid state technology [3].

Thin films play a crucial role in the present day science and technology due to their wide use in a large number of active and passive devices. The characteristic structural and electrical properties of thin films can be tailored by controlling the composition and fabrication processes, e.g. deposition rate, substrate temperature, selection and preparation of substrate, doping, ambient pressure, post deposition annealing [4].

Many workers were obtained Sb_2S_3 thin films by various sophisticated techniques such as electro-deposition [5], dip-dry technique [6], spray pyrolysis [7], chemical bath deposition [8], successive ionic layer adsorption and reaction (SILAR method) [9], the sol-gel method [10] and vacuum evaporation [11-13]. Also, the effect of depositions condition on physical properties of thin films was studied.

Corresponding Author:-N.M. Abdel-Moniem
Address:-Faculty of Science, Tanta University, Egypt.

In this work, the phase transformation, electrical properties and the transition points of Sb_xS_{100-x} were studied using the temperature dependence of electrical conductivity within the range 300-600K.

Experimental procedure:

The bulk Sb_xS_{100-x} chacogenides were prepared by the melt quenching technique (where x=10, 20, 30 and 40 at. %). The desired amounts of the constituent elements (99.999purity) were weighted and then sealed in silica ampoules in vacuum 10^{-5}torr. The sealed ampoules were kept inside electric furnace its temperature raised up to 1100K at a rate 10 degree programmed per minute. Then, the ampoules were maintained at 1100K for 10 hours. During the melt process, the ampoules were agitated frequently to ensure homogenous melt, and were quenched in ice water.

Thin films of the system were prepared by thermal evaporation on to quartz substrates at room temperature. The rate of the films deposition was 5 nm/s. The films thickness ($t \approx 1.2$ μm) was determined using quartz crystal thickness monitor [FTMS] and confirmed interferometrically [13]. The amorphous nature of the thin films was confirmed by X-ray.

The electrical measurements were carried out in a vacuum of 10^{-3}torr in a specially designed sample holder. The electric resistance was measured using two probe methods by Keithley's electrometer. The temperature of the samples was sensed using copper-constantan thermocouple.

Results and Discussions:

Structural Characterizations:

The structure of a-Sb_xS_{100-x} thin films was illustrated by X-ray diffraction (XRD) patterns. Figure (1) represent the XRD in diffraction pattern with diffraction angle ray 10-60^o. This figure shows that the as-deposited sample presents amorphous structures. The films were annealed at 510 K to be agreement with DTA analysis [2]. Since, the DTA analysis gives the glass transition temperature (T_a) and the crystallization temperature (T_c) equal to 490 and 520K, respectively. The main phase of this figure represents Sb_2S_3 thin films as the same [12,13], shown in Table 1. The mean coordination number, Z, is between 2.1 and 2.4 because Sb has three-fold coordinates and S has two-fold coordinates. The average coordination number of covalent bonds, which was measured and represented the structure in atomic units, was calculated; Z=[3x+2(100-x)]/100 where, x is the atomic percentage of Sb [14]. From this relation, it was found that, the coordination number for x=10,20,30 and 40 at % corresponding to Z=2.1, 2.2, 2.3 and 2.4, respectively. Further, for all systems depicted in Figure 1, a gross composition dependence decreases in atomic volume with increasing in the coordination number Z [15]. The assumption of structural transition at Z=2.4 gives a plausible explanation for composition dependence of diffraction peaks intensity as shown in Figure 1. According to the present figure, the intensity increases, reflecting degrees of the two-dimensional correlation. Therefore, the diffraction peak intensity grows continuously from Z=2.1 to 2.4 with the layer evolution. At Z=2.4, the layer structure is fully developed, exhibiting the maximal diffraction peak intensity, which decreases further with increasing the number of cross-linked sites [16]. The peak value of $2\theta=40^o$ is the shortest distance between Sb-S atoms suggesting the triple pyramid, Sb_2S_3, units represent the basic building block of the network structure [17]. The grain size of the peak around $2\theta=40^o$ (Sb_2S_3 phase) was calculated from XRD patterns by using Deby-Scherrer's formula; $L=0.9\lambda/B\cos\theta$, where, B is the full-width at half-maximum (FWHM). It was found that, the grain size of the phase is in the range 56.7-61.4 nm, but the peak intensity of the phase increases with increasing Sb content as shown in Fig.1. In the random-network model of Sb S glasses, the preservation of nearly optimal bond lengths cause fluctuation in the bond angles and Van der Waals distances. These local fluctuations may be large enough to give rise to electronic or vibrational properties quite different from those of the typical bonding configurations in the random-network model. Such fluctuations, then contribute to tails of localized states on the valance and conduction bands [18].

Table 1:- X-ray crystallographic data of a-Sb_xS_{100-x} films after annealing at 510K for 2hrs.

Experimental				ASTM Cards			
Composition x %		2θ	dÅ	Crystal phase	dÅ	hkl	
10	a	16.5	5.3661	S	5.40	002	
	b	18.7	4.7395	S	4.80	202	
	c	24	3.7035	S	3.709	122	
	d	27	3.2629	S	3.258	131,222	
	e	30.2	2.9558	S	2.964	123,231	
	f	34	2.6336	Sb	2.6309	111	Mono-clinic
	g	41.2	2.1885	Sb_2S_3	2.185	331	
	h	45.5	1.9912	Sb_2S_3	1.992	440	
	o	48	1.8931	S	1.8891	610	
	m	52	1.7565	Sb_2S_3	1.754	535	
	n	58.3	1.5808	S	1.622	624	
20	a	24	3.7035	S	3.709	122	
	b	28.6	3.1174	S	3.110	313	
	c	40	2.2513	Sb_2S_3	2.252	430	
	d	42	2.1486	S	2.146	111	
	e	48	1.8931	S	1.900	515	
	f	51.5	1.7724	Sb	1.770	202	Mono-clinic
30	a	24	3.7035	S	3.709	122	
	b	28.6	3.1174	Sb Sb_2S_3	3.1095	102	hexagonal
	c	40	2.2513	Sb_2S_3	2.252	430	
	d	48.5	1.8747	Sb_2S_3	1.871	600	
	e	52	1.7565	S	1.754	535	
	f	54	1.6903		1.6906	132	
40	a	24	3.7035	S	3.709	122	
	b	40	2.2513	Sb_2S_3	2.252	430	
	c	42	2.1486	Sb	2..152	110	
	d	47.3	1.9195	Sb_2S_3	1.920	151	
	e	48.6	1.8711	Sb_2S_3	1.871	600	
	f	51.7	1.7660	Sb	1.770	022	hexagonal

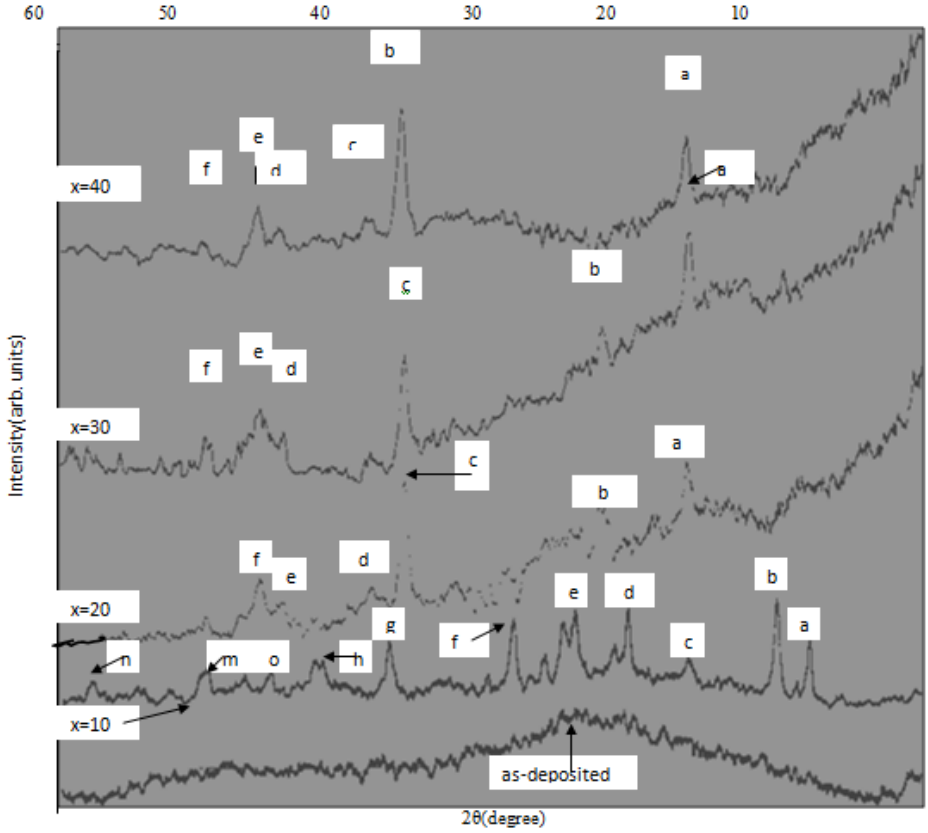

Fig. 1: X-ray diffraction of a- Sb_xS_{100-x} films as-deposited and annealed at 510 K for 2h.

Electrical Properties:

The D.C. conductivity was measured as a function of temperature in the range 300-600 K. The rate of heating is 3-5 K/min., the temperature dependence on conductivity is expressed as;

$$\sigma = \sigma_0 \exp(-\Delta E/kT) \quad (1)$$

Where, σ is the electrical conductivity at absolute temperature T, σ_0 the pre –exponential factor ($\Omega^{-1}cm^{-1}$), k is the Boltezmann constant and ΔE is the activation energy of the free charge carriers. The conductivity during the cooling cycle is closely coincidence to that in the heating cycle [19]. Hence, for all the calculations, the data of the films was done during the heating cycle only. The temperature dependence of electrical conductivity of Sb_xS_{100-x} (where x=10, 20, 30 and 40 at %) films was studied to determine the thermal activation energy during the temperature range mentioned above. Figure 2 represents the D.C. conductivity (ln σ) versus the inverse temperature (1/T). From this figure, it can be seen that the D.C. conductivity increases linearly with increasing the temperature T at different slopes in two domains of temperatures. At high temperature region, the conductivity is increased more than that at low temperature domain. This is due to the transformation of the samples from hopping conductivity to intrinsic semiconductor by increasing the temperature. Accordingly, the activation energy of conduction is changed from narrow hopping gap energy (E_h) to wide activation energy (E_a). This fact shows that, at a certain temperature T_{kink}, the conductivity increases with sharp slope by increasing the temperature T. Two straight lines were obtained confirming the semiconducting behavior as shown in Figure2. The position of T_{kink}depends on Sb content. It has high values of temperature with decreasing Sb content or increasing S content. These phenomena may be due to the presence of localized state in the band gap. Table 2 shows the calculated energies for each region against the atomic percent of Sb. The hopping energy, E_h, decreases with Sb content and increases with S content, in Sb_xS_{100-x} systems. The presence of a hopping regime strongly suggests the important localized states as band tails, that may decrease with decreasing of S content or increasing of Sb content. After annealing at 510K for 2hours, which the crystallization effects are pronounced (Fig. 1), the D.C. conductivity (ln σ) is plotted against 1/T as shown in Figure 3. From this figure, there is a linear relation with one slope during the temperature rang used as mentioned above at a higher percentage of Sb content in the samples. This means that, there is single activation energy for the conductivity. Also, the change of both the activation energy, E_a, and the conductivity values due to crystallization

can be observed. Therefore, the activation energy of the annealed films is lower than that of the as-deposited films, as shown in Table 2. In this table, the activation energies for as-deposited films and annealed films as a function of average coordination number, Z, for all the compositions prepared in Sb_xS_{100-x} films are represented. The results show that, the activation energy decreases with increasing of the average coordination number. In Sb_xS_{100-x} films, with increasing of the average coordination number, the number of Sb-S bonds is decreased then, the average bond energy of the Sb_xS_{100-x} systems is decreased as well [20].

Table 2: The energies for different atomic percent and coordination numbers fora-Sb_xS_{100-x} films.

Composition		10	20	30	40
Coordination number		2.1	2.2	2.3	2.4
As-deposited	E_h(eV)	0.34	0.25	0.22	0.20
	E_a(eV)	0.74	0.51	0.47	0.38
After annealing	E_h(eV)	0.2	0.12	0.11	0.0
	E_a(eV)	0.6	0.42	0.31	0.23

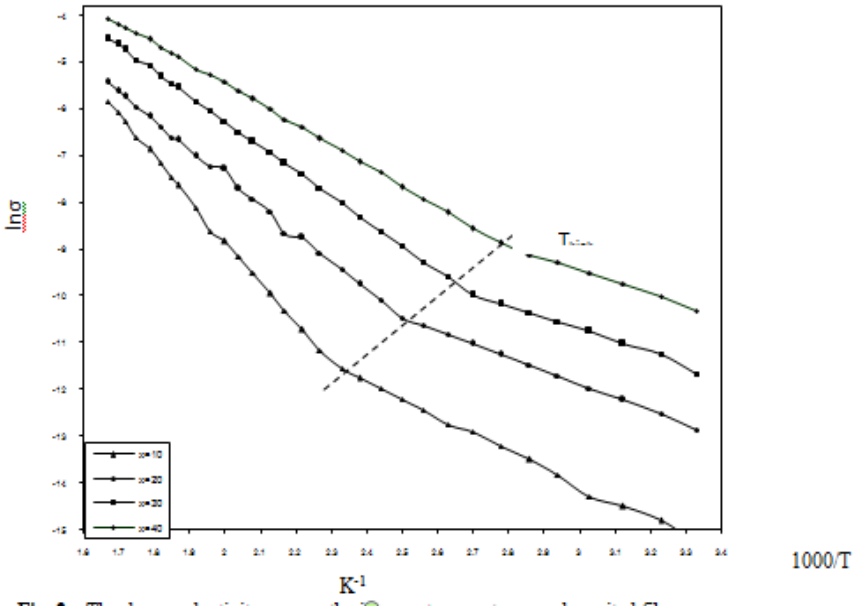

Fig. 2: The d.c. conductivity versus the inverse temperature as-deposited films.

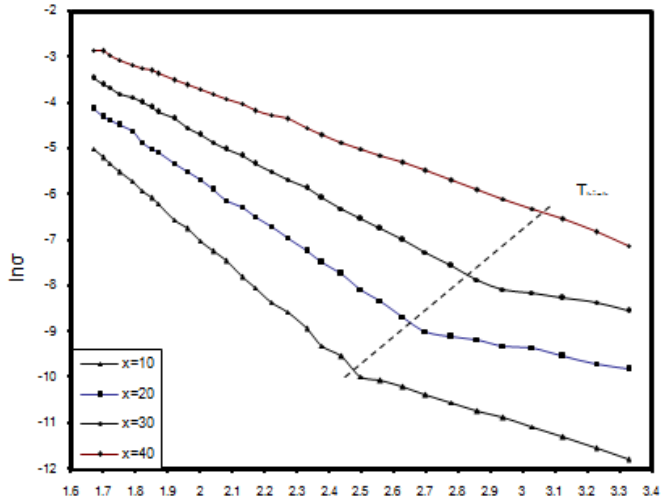

Fig. 3:the d.c. conductivity versus the inverse temperature after annealing films.

Conclusions:

Sb_xS_{100-x} thin films have been deposited onto quartz substrate by thermal evaporation under vacuum 10^{-5}torr. Theas-deposited films were amorphous and annealed at 510K for 2hours. Thermal crystallization and X-ray structure analysis of devitrified materials have been carried out on Sb-S films. These investigations show the following notable features;

The structural analysis revealed that the formation and the properties of as-deposited amorphous Sb_xS_{100-x} films are very sensitive to annealing temperature. The annealed Sb_xS_{100-x} films undergo a structural change from glassy to crystalline forms. It can be related to the phase transitions.

The conductivity measurements for as-deposited amorphous Sb_xS_{100-x} films give a transition temperature T_{kink} from amorphous to crystalline states. The conductivity of annealed films is higher than of as-deposited films due to transition formation of the amorphous films to the crystalline state. After annealing, $Sb_{40}S_{60}$ film gives single activation energy with minimum value (E_a=0.23 eV).

Acknowledgement:

The author wishes to thank Prof. Dr. El-sayed M. Farag who Professor of amorphous semiconductor materials, Basic Science Engineering Department, Faculty of Engineering, Shebin El-Kom, Menoufiya university, Egypt, for his help in electrical properties measurements at his laboratory.

References:

1. RuihongZhang,et al,*Chem. Commun.*, 52(2016), 5007-5010.
2. M.S.Droichi, et al, J. Non-cryst. Solids 101 (1988)151-155.
3. A. U. Ubale, et al, International Journal of Materials and Chemistry 2(4), (2012), 165-172.
4. Nikhil K. Ponon, et al, Thin solid films 2 (2015), 31–37.
5. A. Antenucci, et al, Materials & Design, 71(2015) 78–84.
6. B.B.Nayak, et al, Thin solid films 92, (1982)309.
7. C.H.Bhosal, et al, Thin solid films 249 (1994)137.
8. Mark R. De Guire, et al, Chemical Bath Deposition, Part III, Chp.14(2013)pp 319-339, Springer Vienna.
9. I.K. El Zawawi, et al, Thin solid films 324(1998)300.
10. I.K. El Zawawi, et al, Fizika A7(1998) 97.
11. Z.S. El Mandouh, S.N. Salama, J. Mat. Sci., 25 (1990)1715.
12. N. Tigau, Cryst. Res. Technol., 41, 5(2006)474-480.
13. El-sayed M. Farag,Opt. Mats., 29(2006)397-402.
14. J.C. Phillips, J. Non-cryst. Solids, 34(1979)153.
15. K. Tanaka, Physical review B, 39, 2(1989)1270-1279.
16. K. Tanaka, Philos. Mag. Lett. 7(1988)183.
17. L. Cervinka, A. Hruby, J. Non-cryst. Solids 48(1982)231.
18. El-sayed M. Farag J. Mater. Sci., Mater. Electronics, 15 (2004) 19-23.
19. El-sayed M. Farag, Indian J. phys. 80, 4(2006)367.
20. V. Pamukchieva, et al, J. Non-cryst. Solids, 242(1998)110-114.